

1 **FcγR responses to soluble immune complexes are governed by solubility and size.**

2 Haizhang Chen^{1,2}, Andrea Maul-Pavicic^{3,4}, Martin Holzer⁵, Ulrich Salzer³, Nina Chevalier³, Reinhard E.
3 Voll^{3,4}, Hartmut Hengel^{1,2,#} & Philipp Kolb^{1,2,#}

4 ¹Institute of Virology, University Medical Center, Albert-Ludwigs-University Freiburg, Hermann-Herder-Str. 11, 79104 Freiburg, Germany

5 ²Faculty of Medicine, Albert-Ludwigs-University Freiburg, 79104 Freiburg, Germany

6 ³Department of Rheumatology and Clinical Immunology, Medical Center - University of Freiburg, Faculty of Medicine, University of Freiburg,
7 Hugstetterstr. 55, 79106 Freiburg, Germany

8 ⁴Center for Chronic Immunodeficiency (CCI), Medical Center-University of Freiburg, Faculty of Medicine, University of Freiburg, Breisacherstr.
9 115, 79106 Freiburg, Germany

10 ⁵Institute for Pharmaceutical Sciences, Albert-Ludwigs-University Freiburg, Hermann-Herder-Str. 9, 79104 Freiburg, Germany

11 **#corresponding authors**

12

13 **Summary**

14 This study describes a novel cell-based reporter assay enabling the detection and
15 quantification of soluble multimeric IgG immune complexes (sICs). Receptor triggering of sICs
16 is restricted to specific FcγRs and depends on sIC size. The assay identifies sICs in sera from
17 SLE patients and autoimmune-prone mice as a novel biomarker of autoimmune disease.

18

19 **Abstract**

20 Fcγ-receptor (FcγR) activation by antibody formed soluble immune complexes (sICs) is
21 thought to be a major mechanism of inflammation in certain autoimmune diseases such as
22 systemic lupus erythematosus (SLE). A robust and scalable test system allowing for the
23 detection and quantification of sICs bioactivity is missing. We developed a comprehensive
24 reporter cell panel capable of measuring the sIC-mediated activation of individual human and
25 mouse FcγRs. We show that compared to human FcγRs IIB and III, human FcγRs I and IIA
26 lack sensitivity to sICs. Further, the assay proved to be sensitive to sIC stoichiometry and size
27 enabling us to demonstrate for the first time a complete translation of the Heidelberger-Kendall
28 precipitation curve to FcγR responsiveness. The approach was applied to quantify sICs-
29 mediated FcγR activation using sera from SLE patients and mouse models of lupus and
30 arthritis. Thus, in clinical practice, it might be employed as a test matrix toolbox for FcγR
31 activation evaluating sICs as a biomarker for disease activity in immune-complex mediated
32 diseases.

33

34 **Introduction**

35 Immunoglobulin G (IgG) is the dominant immunoglobulin isotype in chronic infections and in
36 antibody-mediated autoimmune diseases. The multi-faced effects of the IgG molecule rely both
37 on the F(ab) regions, which recognize a specific antigen to form immune complexes (ICs), and
38 the constant Fc region (Fc γ), which is detected by Fc γ receptors (Fc γ Rs) found on most cells
39 of the immune system¹. When IgG binds to its antigen ICs are formed, which, depending on
40 the respective antigen, are either cell-bound or soluble (sICs). The composition of sICs is
41 dependent on the number of epitopes recognized by IgG on a single antigen molecule and the
42 ability of the antigen to form multimers. Fc γ -Fc γ R binding is necessary but not sufficient to
43 activate Fc γ Rs since physical receptor cross-linking generally underlies receptor activation²⁻
44 ⁵. Firmly fixed cell bound ICs are readily able to cross-link Fc γ Rs^{4,6}. This condition induces
45 various signaling pathways⁷⁻⁹ which in turn regulate immune cell effector functions^{10,11}. It is
46 also suggested that sICs can dynamically tune Fc γ R triggering, implying that changes in sIC
47 size directly impact Fc γ R responses⁶. However, the molecular requirements are largely
48 unknown. Also, a functional reproduction of the paradigmatic Heidelberger-Kendall
49 precipitation curve, describing that the molecular size of sICs determined by the
50 antibody:antigen ratio dynamically tunes Fc γ R activation on and off^{12,13}, is so far missing.
51 In contrast to Fc γ R binding of monomeric ligands without consequences, IC-mediated Fc γ R
52 cross-linking initiates the full signal cascade followed by immune cell activation or inhibition,
53 resp.^{5,8,14,15}. Human Fc γ Rs are membrane resident receptors recognizing Fc γ . Among all
54 type I Fc γ Rs, Fc γ RIIB (CD32B) is the only inhibitory one signaling via immunoreceptor
55 tyrosine-based inhibitory motifs (ITIMs) while the activating receptors are associated with
56 immunoreceptor tyrosine-based activation motifs (ITAMs). Another exception is Fc γ RIIIB
57 (CD16B), which is glycosylphosphatidylinositol (GPI)-anchored¹⁶⁻¹⁹. Fc γ RI (CD64) is the only
58 receptor with high affinity binding to monomeric IgG not associated with antigen and is primarily
59 tasked with phagocytosis linked to antigen processing and pathogen clearance^{20,21}. All the
60 other Fc γ Rs only efficiently bind to complexed, meaning antigen-bound IgG^{1,16,17}. While
61 Fc γ RI, Fc γ RIIB and Fc γ RIIIA are able to recognize sICs, this has not been reported for Fc γ RIIA

62 (CD32A), rather this receptor has recently been shown to depend on the neonatal Fc receptor
63 (FcRn) to do so ^{22, 23}.

64 Activation of FcγRs leads to a variety of cellular effector functions such as antibody-dependent
65 cellular cytotoxicity (ADCC) by natural killer (NK) cells via FcγRIIIA, antibody-dependent
66 cellular phagocytosis (ADCP) by macrophages via FcγRI, cytokine and chemokine secretion
67 by NK cells and macrophages via FcγRIIIA. Further effector responses are reactive oxygen
68 species (ROS) production of neutrophils and neutrophil extracellular traps formation (NETosis)
69 via FcγRIIIB, dendritic cell (DC) maturation and antigen presentation via FcγRIIA and B cell
70 selection and differentiation via FcγRIIB ^{10, 24-30}. Consequently, FcγRs connect and regulate
71 both innate and adaptive branches of the immune system. Various factors have been indicated
72 to influence the IC-dependent FcγR activation profiles, including Fcγ-FcγR binding affinity and
73 avidity ³¹, IgG subclass, glycosylation patterns and genetic polymorphism ^{4, 24, 25, 32},
74 stoichiometry of antigen-antibody-ratio ^{6, 30, 33} and FcγR clustering patterns ³⁴. Specifically,
75 Asn297-linked glycosylation patterns of the IgG Fc domain initiate either pro- or anti-
76 inflammatory effector pathways by tuning the binding affinity to activating versus inhibitory
77 FcγRs, respectively ³⁵. However, despite being explored in proof-of-concept studies, the
78 functional consequences of these ligand features on a specific receptor are still not fully
79 understood. Therefore, an assay platform allowing for the systematic functional assessment
80 of IC-mediated FcγR activation is strongly required. sICs and immobilized ICs represent
81 different stimuli for the immune system ^{22, 29}. Soluble circulating ICs are commonly associated
82 with certain chronic viral or bacterial infections ^{36, 37} and autoimmune diseases, such as
83 systemic lupus erythematosus (SLE) or rheumatoid arthritis (RA) ³⁸⁻⁴⁰. When accumulating and
84 deposited in tissues sICs can cause local damage due to inflammatory responses, classified
85 as type III hypersensitivity ⁴¹. Typically, sICs related disorders are characterized by systemic
86 cytokine secretion which can be followed by immune cell exhaustion and senescence ^{42, 43}. In
87 order to study sIC-dependent activation of FcγRs in detail, we employed a cell-based assay
88 which has been previously utilized to study immobilized ICs ⁴⁴ and adapted it into a sIC
89 sensitive reporter system capable of distinguishing the activation of individual FcγRs and their

90 responses to varying complex size. This approach allowed for the first time a complete
91 reproduction of the Heidelberger-Kendall precipitation curve measuring actual FcγR triggering.
92 The assay enables a quantification of clinically relevant sICs in sera from SLE patients and
93 autoimmune-prone mice with immune-complex-mediated arthritis and lupus using reporter
94 cells expressing chimeric mouse FcγRs.

95

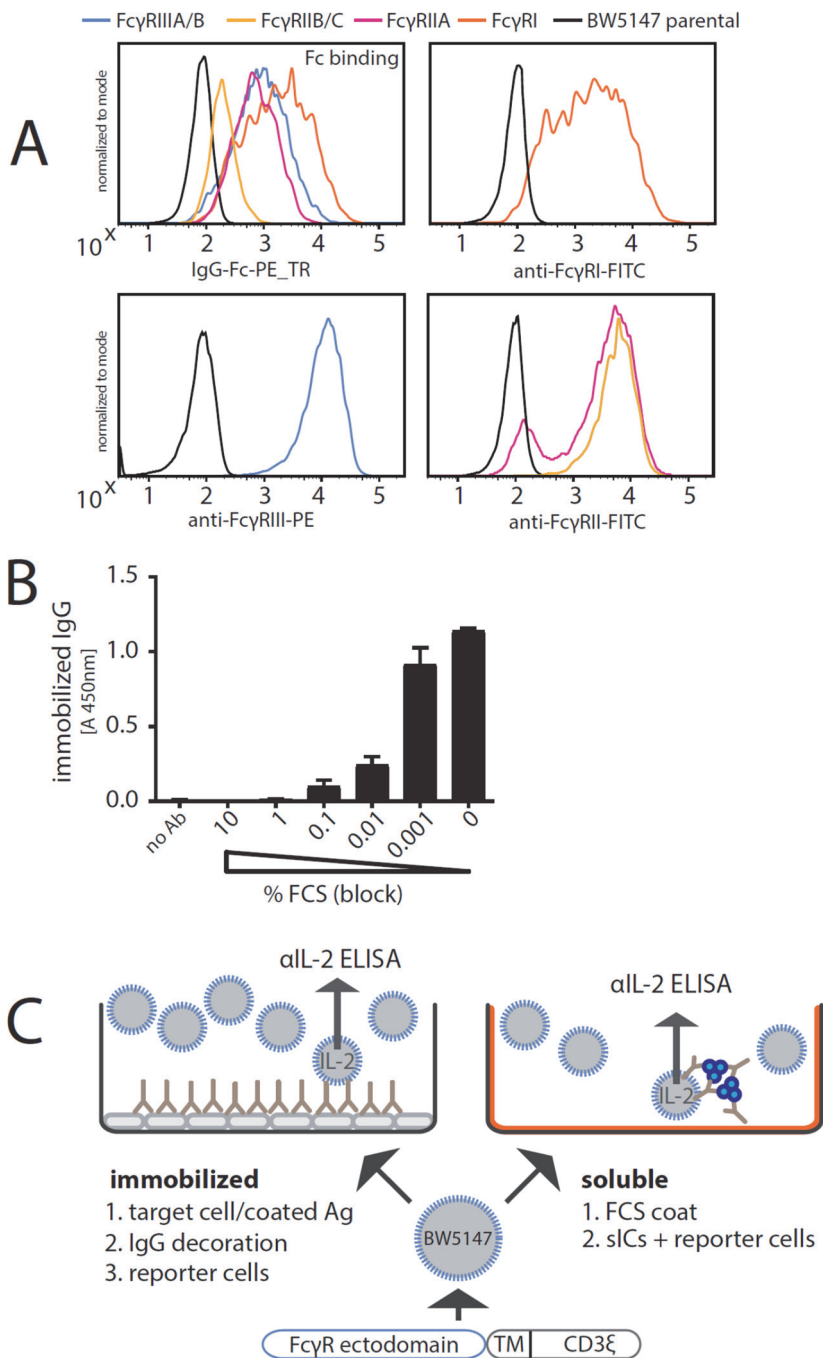
96 **Results**

97

98 **Experimental assay setup**

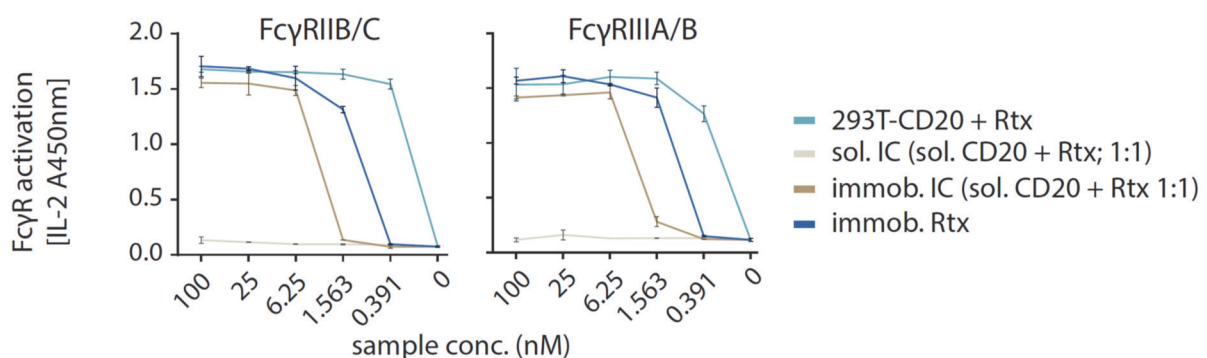
99 The assay used in this study was adapted from a previously described cell-based FcγR
100 activation assay designed to measure receptor activation in response to opsonized virus
101 infected cells ⁴⁴ or therapeutic Fc-fusion proteins ⁴⁵. We complemented the assay setup to
102 enable measurement of sICs when incubated with reporter cells stably expressing the
103 ectodomains of the human FcγR fused to the signaling module of the mouse CD3-ζ chain
104 (FcγRI: Acc# LT744984; FcγRIIA(R): Acc# M28697; FcγRIIB/C: Acc# LT737639;
105 FcγRIIIA/B(V): Acc# LT737365). Ectodomains of FcγRIIIA and FcγRIIIB as well as
106 ectodomains of FcγRIIB and FcγRIIC are identical. Second generation reporter cells were
107 generated to improve stable expression of chimeric FcγRs compared to the transfectants used
108 in the original assay ⁴⁴. To this end, BW5147 cells were transduced as described previously
109 via lentiviral transduction ^{44, 46}. Human FcγR expression on transduced cells after puromycin
110 selection is shown in Fig. 1A. FcγR triggering is translated into activation of the reporter cells
111 and measured by quantification of endogenous IL-2 (mIL-2) secretion into the cell culture
112 supernatant using an anti-IL-2 sandwich ELISA as described previously ⁴⁴. In order to employ
113 the original assay, designed to detect ICs on adherent virus-infected cells, for the detection of
114 soluble ICs we first determined the suspension of IgG achieved by pre-incubating a 96 well
115 ELISA microtiter plate with PBS/FCS blocking buffer. To this end, we compared graded
116 concentrations of FCS in the blocking reagent and measured the threshold at which IgG
117 (rituximab, Rtx) was no longer adsorbed to the plate and stayed abundantly in solution. Fig.

118 1B demonstrates that FCS supplementation to 1% (v/v) or higher is sufficient to keep IgG
 119 antibodies in solution and prevents binding to the plastic surface. Using this adapted protocol,
 120 the assay now allowed for the sensitive detection and characterization of FcγR interaction with
 121 immobilized ICs versus sICs as shown schematically in Fig. 1C. First, we set out to test if
 122 monomeric IgG upon immobilization becomes an operational surrogate for IgG-opsonized cells
 123 or immobilized ICs with regard to FcγR activation as suggested before ⁴⁷.



127 or BW5147 parental cells were stained with Fc γ R specific conjugated mAbs as indicated and
128 measured for surface expression of Fc γ Rs via flow cytometry. Fc γ binding was determined
129 using a PE-TexasRed-conjugated human IgG-Fc fragment. B) FCS coating of an ELISA
130 microtiter plate allows for suspension of subsequently added IgG. Plate bound IgG was
131 quantified via ELISA. PBS supplemented with >1% FCS (v/v) avoids adhesion of IgG
132 (rituximab, Rtx) to the ELISA plate. C) Schematic of an immobilized IC or soluble IC setup.
133 BW5147 reporter cells expressing chimeric human Fc γ R receptors secrete IL-2 in response to
134 Fc γ R activation by clustered IgG. Soluble ICs are generated using mAbs and multivalent
135 antigens (blue). Solubility is achieved by pre-blocking an ELISA plate using PBS supplemented
136 with 10% FCS (FCS coat, orange).
137 As depicted in Fig. 2, there was no qualitative difference in Fc γ R activation between
138 immobilized Rtx, immobilized ICs (Rtx + rec. CD20) or Rtx-opsonized 293T-CD20 cells,
139 showing that Fc γ R cross-linking by clustered IgG alone is sufficient for receptor cross-linking
140 and activation. In contrast, sICs formed by monomeric CD20 peptide (aa 141-188) and Rtx
141 failed to activate Fc γ Rs even at very high ligand concentrations. Based on this finding we
142 hypothesized that, in order to generate sICs able to activate Fc γ Rs, antigens have to be
143 multivalent to achieve cross-linking of Fc γ Rs. Of note, to reliably and accurately differentiate
144 between soluble and immobilized triggers using this assay, reagents for the generation of ICs
145 need to be of very high purity and consistent stability. Indeed, only combinations of
146 pharmaceutical therapy grade, i.e. ultra-pure mAbs and pure antigens (purified via size
147 exclusion chromatography) showed reproducible, dose-dependent and specific activation in
148 the reporter assay (data not shown).

149



150

151 **Fig. 2. Fc γ RIIB/C and Fc γ RIIIA/B do not respond to small hetero-dimeric sICs but are**
152 **sensitive to immobilized IgG/ICs.** Dose-dependent activation of Fc γ R-bearing reporter cells
153 by immobilized IC can be mimicked by immobilized IgG. Response curves of human Fc γ RIIB/C
154 and Fc γ RIIIA/B are similar between opsonized cells (293T cells stably expressing CD20 + Rtx),
155 immobilized IC (rec. soluble CD20 + Rtx) and immobilized IgG (Rtx). sIC formed by monovalent

156 antigen (rec. soluble CD20) do not activate human FcγRs. X-Axis shows sample concentration
157 determined by antibody molarity. Y-Axis shows FcγR activation determined by reporter cell IL-
158 2 production.

159

160 **Quantification of human FcγR responsiveness to multimeric sICs**

161 To date, there are only few commercially available human IgG-antigen pairs that meet both
162 the above mentioned high grade purity requirements while also providing a multimeric antigen.

163 In order to meet these stipulations of ultra-pure synthetic soluble immune complexes we

164 focused on three pairs of multivalent antigens and their respective mAbs that were available

165 in required amounts enabling large-scale titration experiments; trimeric rhTNFα:IgG1 infliximab

166 (TNFα:Ifx), dimeric rhVEGFA: IgG1 bevacizumab (VEGFA/Bvz) and dimeric rhIL-5: IgG1

167 mepolizumab (IL-5/Mpz). As lymphocytes express TNFα-receptors I and II while not

168 expressing receptors for IL-5 or VEGFA, we tested whether the mouse lymphocyte derived

169 BW5147 thymoma reporter cell line is sensitive to high concentrations of rhTNFα. Toxicity

170 testing revealed that even high concentrations up to 76.75 nM rhTNFα did not affect viability

171 of reporter cells (Fig. S1). Next, we measured the dose-dependent activation of human FcγRs

172 comparing immobilized IgG to soluble ICs using the FcγR reporter cell panel (Fig. 3). Soluble

173 antigen or mAb alone served as negative controls showing no background activation even at

174 high concentrations. Immobilized rituximab served as a positive control for inter-experimental

175 reference. We observed that all FcγRs are strongly activated in a dose-dependent manner

176 when incubated with immobilized IgG. Incubating the FcγR reporter cells with sICs at identical

177 molarities showed FcγRIIB/C and FcγRIIIA/B to be efficiently activated by sICs, while in

178 contrast, FcγRIIA and FcγRI did not respond to sICs. We furthermore observed FcγRIIIA/B to

179 be efficiently activated by sICs with responses even surpassing those achieved with

180 immobilized IgG for TNFα/Ifx and IL-5/Mpz ICs. FcγRIIB/C showed a generally weaker

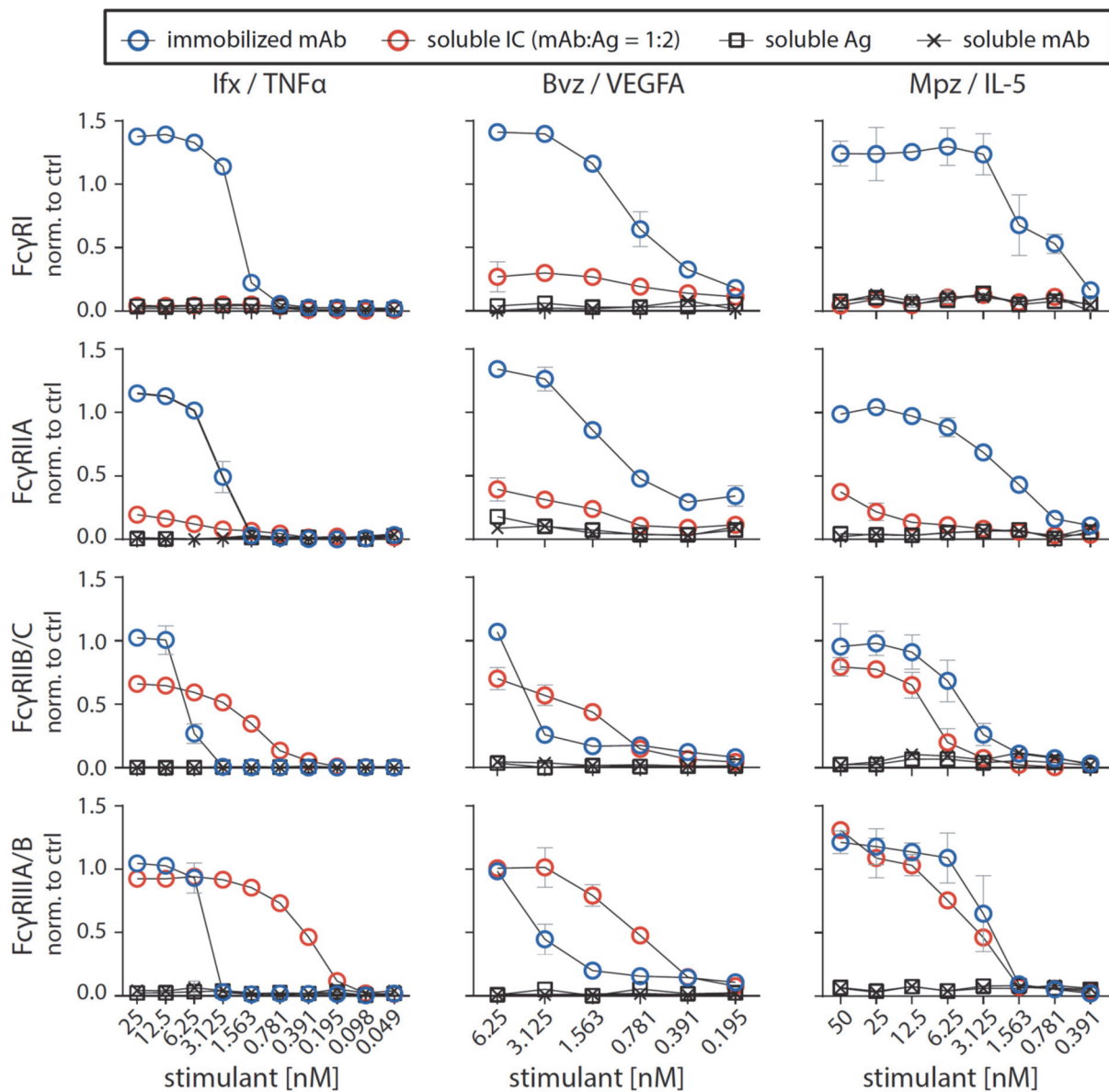
181 reactivity towards sICs compared to immobilized ICs, especially at high concentrations

182 whereas an inversion of this order was seen for TNFα/Ifx and VEGFA/Bvz ICs at lower

183 concentrations. IL-5/Mpz, FcγRIIB/C and FcγRIIIA/B showed similar responsiveness towards

184 immobilized or sICs with a generally stronger activation on immobilized ICs. These findings

185 demonstrate that sICs of different composition vary in the resulting FcγR activation pattern,
 186 most likely due to the antigens being either dimeric, trimeric or different in size.

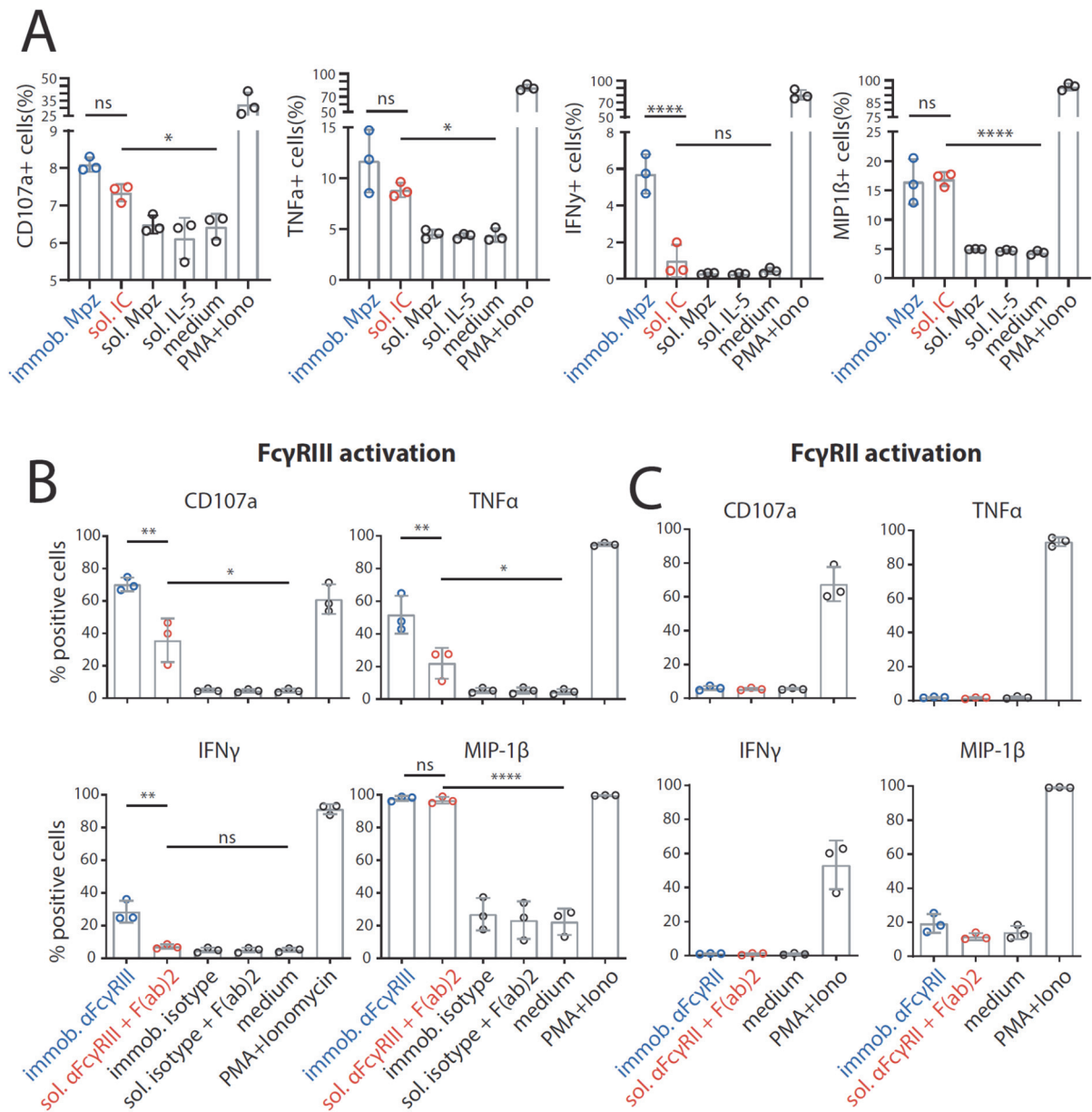


187

188 **Fig. 3. FcγRIIB/C and FcγRIIIA/B are activated by sICs formed from multivalent antigens.**

189 Three different multivalent ultra-pure antigens (Ag) mixed with respective therapy-grade mAbs
 190 were used to generate sICs as indicated for each set of graphs (top to bottom). IC pairs:
 191 infliximab (Ifx) and rhTNFα; mepolizumab (Mpz) and rhIL-5; bevacizumab (Bvz) and rhVEGFA.
 192 X-Axis: concentrations of stimulant expressed as molarity of either mAb or Ag monomer and
 193 IC (expressed as mAb molarity) at a mAb:Ag ratio of 1:2. Soluble antigen or soluble antibody
 194 alone served as negative controls and were not sufficient to activate human FcγRs. FcγR
 195 responses were normalized to immobilized rituximab (Rtx) at 1μg/well (set to 1) and a medium
 196 control (set to 0). All FcγRs show dose-dependent activation towards immobilized IgG. FcγRIIA
 197 shows low activation at high sIC concentrations compared to immobilized IgG activation. FcγRI
 198 shows no activation towards sICs. FcγRIIIA/B and FcγRIIB/C are dose-dependently activated
 199 by sICs with responses comparable in strength to immobilized IgG stimulant. Experiments

200 performed in technical replicates. Error bars = SD. Error bars smaller than symbols are not
201 shown.
202
203 As we observed differences in responses to sICs vs. immobilized ICs for individual FcγR-ζ
204 reporter cells, this indicates that FcγR ectodomains alone are already able to differentiate
205 between these triggers. To validate this observation in principle, we determined FcγRIIIA
206 activation using primary human NK cells isolated from PBMCs of healthy donors. NK cells were
207 chosen as they mostly express only one type of FcγR similar to our reporter system. Measuring
208 a panel of activation markers and cytokine responses by flow cytometry, we observed a
209 differential activation pattern depending on ICs being soluble or immobilized at equal molarity
210 (Fig. 4A). We chose IL-5/Mpz sICs as NK cells do not express the IL-5 receptor. While MIP1-
211 β responses were comparable between the two triggers, degranulation (CD107a) and TNFα
212 responses showed a trend towards lower activation by sICs compared to immobilized IgG
213 (Mpz). Strikingly, IFNγ responses were significantly weaker when NK cells were incubated with
214 sICs compared to immobilized IgG. In order to confirm this hierarchy of responses and to
215 enhance the overall low activation by Fcγ compared to the PMA control, we changed the IC
216 setup by generating reverse-orientation sICs consisting of human FcγR-specific mouse mAbs
217 and goat-anti-mouse IgG F(ab)₂ fragments. NK cell activation by reverse sICs was compared
218 to NK cell activation by immobilized FcγR specific mAbs (Fig. 4B). Here, we not only confirm
219 our previous observations regarding MIP-1β and IFNγ, but we also confirm significantly lower
220 TNFα and CD107a responses towards soluble complexes compared to immobilized mAbs.
221 Importantly, these experiments validate that sICs readily activate primary NK cells and induce
222 immunological effector functions. As in roughly 10% of the population NK cells express
223 FcγRIIC⁴⁸⁻⁵¹, we also tested if this receptor plays a role in our measurements. Using the same
224 three donors and an FcγRII specific mAb as described above, we did not observe an FcγRII-
225 mediated response. Accordingly, we conclude that FcγRIIC expression did not play a role in
226 our experiments (Fig. 4C). Taken together, we show that multivalent but not dimeric soluble
227 immune complexes govern primary NK cell response and FcγRIIIA/B activation (Fig. 2A).



228

229 **Fig. 4. The FcγRIII-dependent activation pattern of primary NK cells depends on IC**
 230 **solubility.** Negatively selected primary NK cells purified from PBMCs of three healthy donors
 231 were tested for NK cell activation markers. Error bars = SD. Two-way ANOVA (Turkey). A) NK
 232 cells were incubated with immobilized IgG (mepolizumab, Mpz), soluble IC (Mpz:IL-5 = 1:1),
 233 soluble Mpz or soluble IL-5 (all at 200 nM, 10⁶ cells). Incubation with PMA and Ionomycin (Iono)
 234 served as a positive control. Incubation with medium alone served as a negative control. B)
 235 NK cells were incubated for 4 h with immobilized FcγRIII-specific mAb, soluble mouse-anti-
 236 human IgG F(ab)₂ complexed FcγRIII-specific mAb (reverse sICs), immobilized IgG of non-
 237 FcγRIII-specificity (isotype control) or soluble F(ab)₂ complexed isotype control (all at 1 μg, 10⁶
 238 cells). Incubation with PMA and Ionomycin served as a positive control. Incubation with
 239 medium alone served as a negative control. C) As in B using an FcγRII-specific mAb. NK cells
 240 from the tested donors in this study do not react to FcγRII activation.

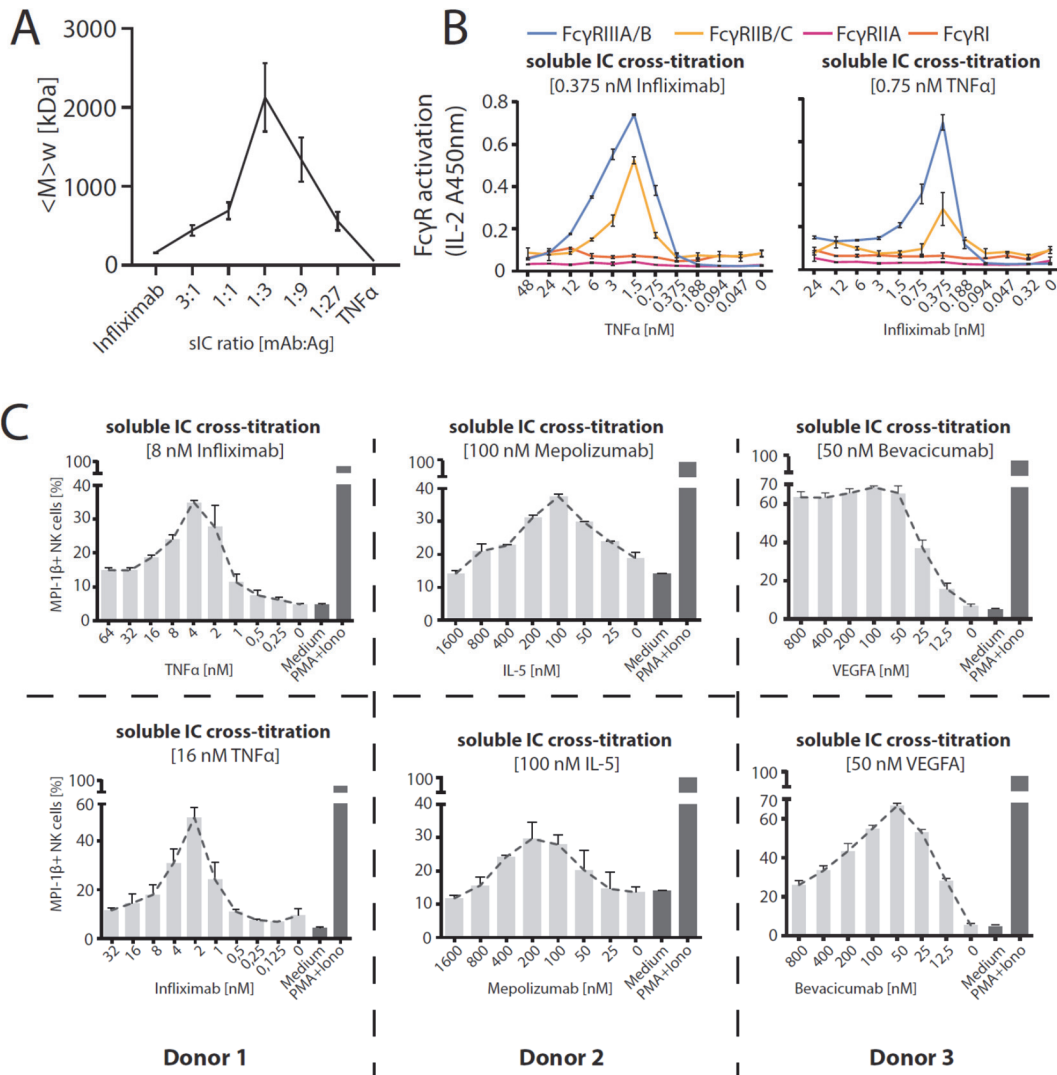
241

242

243 **Measurement of FcγR activation in response to changing sIC size.**

244 We observed that the dimeric sIC CD20:Rtx molecule complex completely failed to trigger
245 FcγRs, while potentially larger sICs based on multimeric antigens showed an efficient dose-
246 dependent FcγR activation. In order to determine whether BW5147 FcγR-ζ reporter cells are
247 able to respond to changes in sIC size, we tested cross-titrated amounts of antibody (mAb,
248 infliximab, Ix) and antigen (Ag, rhTNFα). To this end, the reporter cells were incubated with
249 sIC of different mAb:Ag ratios by fixing one parameter and titrating the other. According to the
250 Heidelberger-Kendall precipitation curve¹² describing sIC size as being dependent on the
251 mAb:Ag ratio, this should result in varying sIC sizes as an excess of either antigen or antibody
252 results in the formation of smaller complexes compared to the large molecular complexes
253 formed at around equal molarity. Changes in sIC size due to a varying mAb:Ag ratio were
254 quantified using asymmetrical flow-field flow fractionation (AF4) (Fig. 5A and Table S1). Fig.
255 S2 shows a complete run of such an analysis. AF4 analysis identifies the highest sIC mean
256 molecular being approximately 2130 kDa at a 1:3 ratio (mAb Ix : Ag TNF-α) with sICs getting
257 smaller with increasing excess of either antigen or antibody, recapitulating a Heidelberger-
258 Kendall-like curve. Incubation of the FcγR reporter cells with ICs of varying size indeed shows
259 that the assay is sensitive to exactly monitor changes in sIC size (Fig. 5B). Accordingly, both
260 FcγR types showed the strongest responses at mAb:Ag ratios of approximately 1:3. We then
261 set out to test the accuracy of our reporter cell assay as a surrogate for primary human immune
262 cells expressing FcγRs. To this end, we tested primary NK cells from three individual donors
263 and measured NK cell MIP1-β upregulation in response to synthetic sICs of varying size and
264 composition again using a similar assay setup optimized for NK cell activation. We chose MIP-
265 1β upregulation as a cell surface marker to measure NK cell activation as it showed the highest
266 responsiveness in previous experiments (Fig. 4). We could observe that primary immune cells
267 expressing FcγRIIIA respond to IC size, confirming our assay to be an accurate surrogate for
268 primary immune cell responses to soluble ICs (Fig. 5C). Convincingly, NK cell responses to
269 sICs generated from trimeric antigen (rhTNFα) peaked at a different mAb:Ag ratio compared
270 to NK cell responses to sICs generated from dimeric antigens (rhIL-5 and rhVEGFA). Of note,

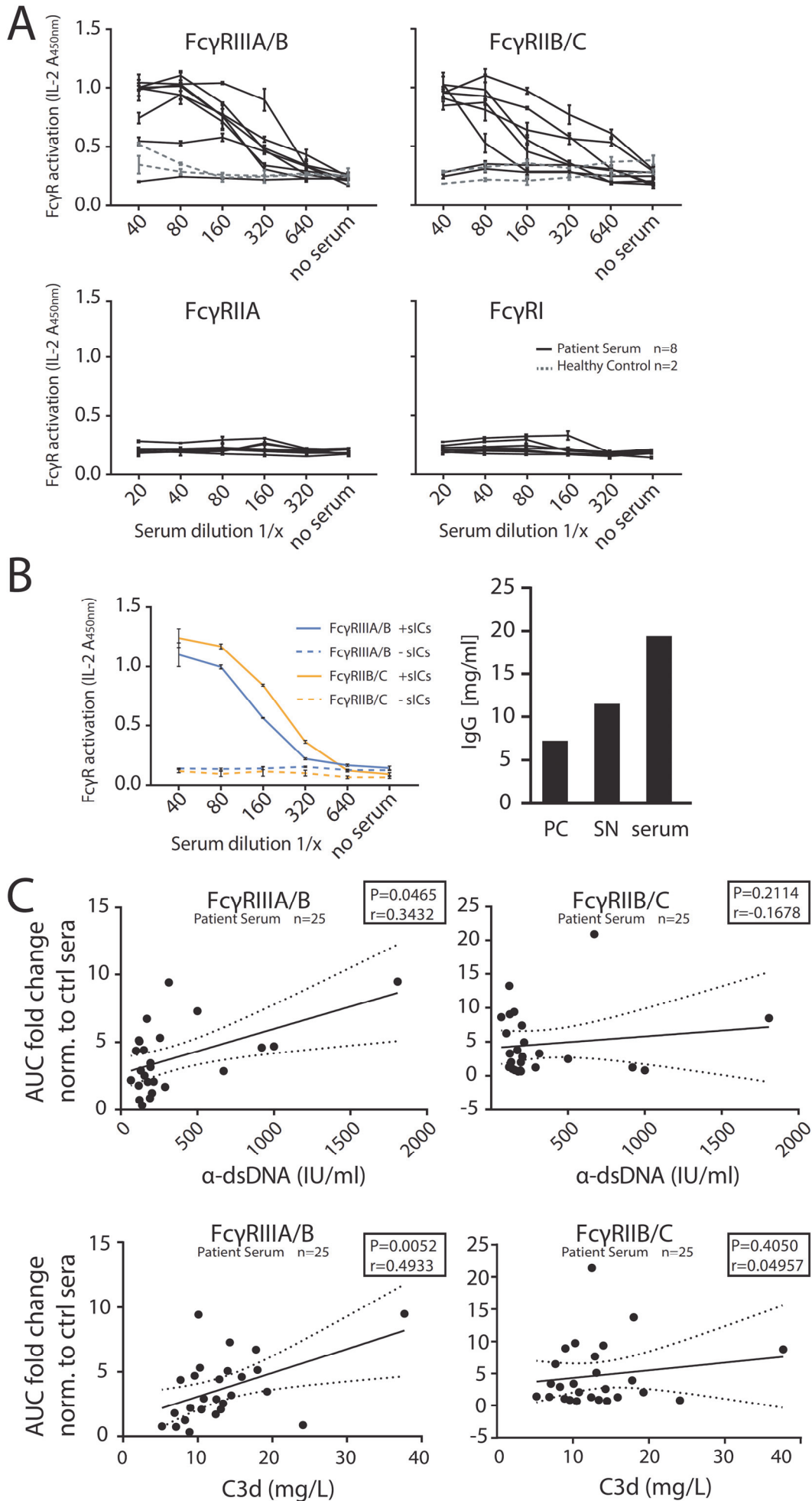
271 TNF α and VEGFA activate resting NK cells thus leading to higher MIP1- β positivity when NK
272 cells are incubated in the presence of excess antigen. As NK cells do not express IL-5 receptor,
273 this effect is not observed in the presence of excess IL-5. Regarding TNF α , NK cells still show
274 a stronger activation by sICs generated under optimal mAb:Ag ratios compared to conditions
275 where excess antigen is used. The data reveal a direct correlation between sIC size and
276 effector responses. Conversely, when changing antibody concentrations using fixed amounts
277 of antigen, a consistent reduction of NK cell activation is observed in the presence of excess
278 IgG for all three mAb/Ag pairs.
279



280

281 **Fig. 5. FcγRIIIB/C and FcγR-III A/B respond to sIC size reproducing a Heidelberger-**
 282 **Kendall like precipitation curve.** A) infiximab (mAb) and rhTNFα (Ag) were mixed at different
 283 ratios (17 μg total protein, calculated from monomer molarity) and analysed via AF4. sIC size
 284 is maximal at a 1:3 ratio of mAb:Ag and reduced when either mAb or Ag are given in excess.
 285 $\langle M \rangle_w$ = mass-weighted mean of the molar mass distribution. Three independent experiments.
 286 Error bars = SD. Data taken from Table S1. One complete run analysis is shown in Fig. S2. B)
 287 FcγR BW5147 reporter cell activation is sensitive to sIC size. sICs of different size were
 288 generated by cross-titration according to the AF4 determination. Reporter cells were incubated
 289 with fixed amounts of either mAb (infiximab, left) or Ag (rhTNFα, right) and titrated amounts of
 290 antigen or antibody, respectively. X-Axis shows titration of either antigen or antibody,
 291 respectively (TNFα calculated as monomer). IL-2 production of reporter cells shows a peak for
 292 FcγRIIIB/C and FcγRIIIA/B activation at an antibody:antigen ratio between 1:2 and 1:4. FcγRs
 293 I and IIA show no activation towards sICs in line with previous observations, see Fig.3. Two
 294 independent experiments. Error bars = SD. C) Primary NK cells purified by negative selection
 295 magnetic bead separation from three different donors were incubated with cross-titrated sICs
 296 as in A. NK cells were measured for MIP-1β expression (% positivity). Incubation with PMA
 297 and Ionomycin served as a positive control. Incubation with medium alone served as a negative
 298 control. Measured in technical replicates. Error bars = SD.
 299 **Quantification of sIC bioactivity in sera of SLE patients.**

300 In order to apply the assay to a clinically relevant condition associated with the occurrence of
301 sICs we measured circulating sICs present in the serum of SLE patients with variable disease
302 activity. Sera from 4 healthy donors and 25 SLE patients were investigated for FcγRIIIA/B and
303 FcγRIIB/C activation. Reporter cells readily produced IL-2 in response to patient sera in a dose-
304 dependent manner (shown exemplarily for some SLE patients, see Fig. 6A), which was not the
305 case when sera from healthy controls were tested. Consistent with the observation that FcγRI
306 and FcγRIIA do not respond to synthetic sICs, reporter cells expressing these receptors did
307 also not respond to the tested serum samples (Fig. 6A, lower panel). While this reaction pattern
308 already indicated that sICs are the reactive component measured in SLE patients' sera, we
309 further demonstrate that FcγRIIIA/B and FcγRIIB/C activation depends on the presence of
310 serum ICs by analyzing patient serum before and after polyethylene glycol (PEG) precipitation
311 and depletion of sICs (Fig. 6B). Next, we calculated the area under the curve (AUC) values for
312 all 25 SLE patient titrations and normalized them to the AUC values measured for healthy
313 individuals. The resulting index values were then correlated with established biomarkers of
314 SLE disease activity, such as anti-dsDNA titers (α -dsDNA) and concentrations of the
315 complement cleavage product C3d (Fig. 6C). We observed a significant correlation between
316 our FcγRIIIA/B activation index values and both of the determined disease activity markers,
317 anti-dsDNA titers and C3d concentration ($p=0.0465$ and $p=0.0052$, respectively). FcγRIIB/C
318 on the other hand showed no significant correlation with either biomarker. We assume these
319 interrelations may be due to the influence of IgG sialylation found to be reduced in active SLE
320 ⁵². Generally, de-sialylation of IgG leads to stronger binding by the activating receptors FcγRI,
321 FcγRIIA and FcγRIII while it reduces the binding affinity of the inhibitory FcγRIIB ⁵³. In sum,
322 our assay allows the indirect quantification of clinically relevant sICs in sera of SLE patients.

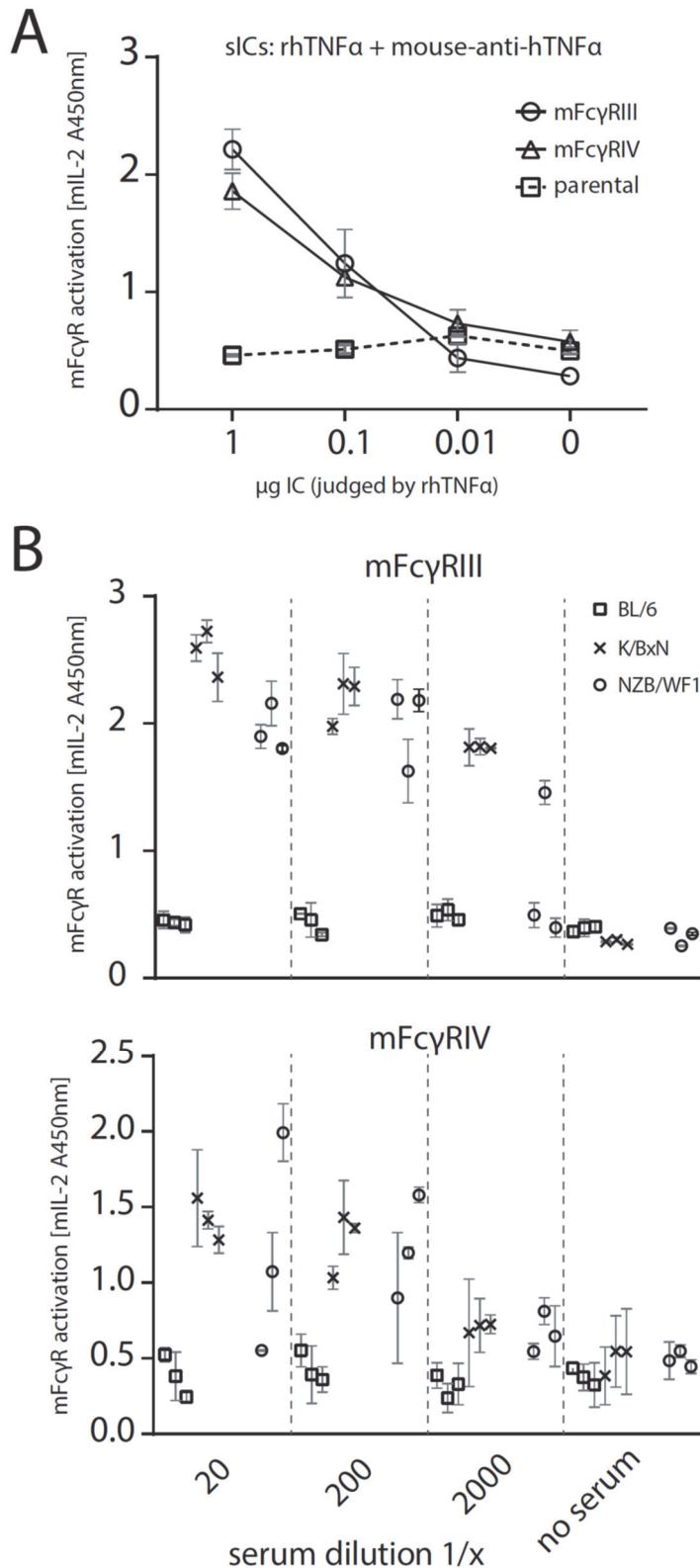


324 **Fig. 6. The reporter assay enables quantification of serum-derived sICs from SLE**
325 **patients.** Serum derived sIC from systemic lupus erythematosus (SLE) patients activate
326 human FcγR reporter cells. 25 patients and 4 healthy control individuals were separated into
327 three groups for measurement. A) Experiments shown for an exemplary group of 8 SLE
328 patients and two healthy individuals. Dose-dependent reactivity of FcγRs IIIA/B and IIB/C was
329 observed only for SLE patient sera and not for sera from healthy individuals. FcγRs I and IIA
330 show no reactivity towards clinical IC in line with previous observations. B) Activation of FcγRs
331 IIB/C and IIIA/B by patient serum is mediated by serum derived sICs. Patient serum samples
332 were depleted of sICs by PEG precipitation and the supernatant (SN) was compared to
333 untreated serum regarding FcγR activation (left). Performed in technical replicates. IgG
334 concentration in the precipitate (PC), supernatant (SN) or unfractionated serum respectively is
335 shown in the bar graph (right). IC precipitation did leave non-complexed IgG in the supernatant.
336 C) FcγRIIIA/B activation, but not FcγRIIB/C activation, significantly correlates with known SLE
337 disease markers. FcγR activation data from A was correlated to established SLE disease
338 markers (α -dsDNA levels indicated as IU/ml or C3d concentrations indicated as mg/L). FcγR
339 activation from a dose-response curve as in A was calculated as area under curve (AUC) for
340 each SLE patient (n=25) or healthy individual (n=4) and expressed as fold change compared
341 to the healthy control mean. SLE patients with α -dsDNA levels below 50 IU/ml and C3d values
342 below 6 mg/L were excluded. One-tailed Spearman's.
343

344 **Assay application to clinically relevant *in vivo* lupus and arthritis mouse models.**

345 BW5147 reporter cells stably expressing chimeric mouse as well as rhesus macaque FcγRs
346 have already been generated using the here described methodology and were successfully
347 used to measure FcγR activation by opsonized adherent cells in previous studies^{46, 54} (mFcγR
348 reporter cells). As the human FcγR reporter cells described here are sensitive to certain sICs,
349 we next aimed to translate the assay to clinically relevant animal models. To this end, we
350 incubated previously described FcγR reporter cells expressing chimeric mouse FcγRs⁴⁶ with
351 sera from lupus (NZB/WF1) or arthritis (K/BxN) mice with active autoimmune disease. The
352 reporter assay was performed as described above. We chose to measure the stimulation of
353 the activating receptors, mFcγRIII and mFcγRIV, that correspond to human FcγRIII and show
354 a similar cellular distribution and immune function¹⁶. Incubation with synthetic sICs generated
355 from rhTNF α and mouse-anti-hTNF α IgG1 showed both of the mFcγR reporter cells to be
356 equally responsive to sICs (Fig. 7A). Parental BW5147 cells expressing no FcγRs served as a
357 control. The sera of three mice per group were analysed and compared to sera from wildtype
358 C57BL/6 mice, which served as a healthy control. C57BL/6 mice were chosen, as healthy
359 K/BxN or NZB/WF1 mice cannot be reliably defined. This is due to the unpredictable disease

360 progression in these mouse models starting from a young age. We consistently detected
361 mFcγR activation by sera from K/BxN or NZB/WF1 compared to C57BL6 mice (Fig. 7B). While
362 the mFcγRIII responses were generally high and similar between K/BxN and NZB/WF1 mice,
363 mFcγRIV responsiveness attended to be lower and individually more variable. Altogether, the
364 assay enables the reliable detection of sICs in sera of mice with immune-complex mediated
365 diseases making it a promising novel tool to monitor sICs as a biomarker of disease activity.



366

367 **Fig. 7. The reporter assay can be applied to mouse models of autoimmune disease.** A)
368 Reporter cells expressing mFcγRIII, mFcγRIV or parental BW5147 cells were incubated with
369 titrated amounts of synthetic sICs generated from rhTNF α and mouse-anti-hTNF α at a 1:1 ratio
370 by mass. One experiment in technical replicates. Error bars = SD. B) Titrations of 3 mouse
371 sera per group (C57BL/6, K/BxN or NZB/WF1) were incubated with mFcγR reporter cells and
372 FcγR activation was assessed as described above. Sera from BL/6 mice served as negative
373 control. Performed in technical replicates. Error bars = SD.

374 **Discussion**

375

376 In this study we established, validated and applied a new assay system that is able for the first
377 time to selectively detect soluble multimeric immune complexes as discrete ligands of FcγR.
378 Major findings are i) that sICs cross-link and trigger human FcγRs IIB/C and IIIA/B but are
379 neglected by activating FcγRI and IIA; ii) that sICs potency is strictly stoichiometry- and size-
380 dependent and thus reproducing the classical Heidelberger-Kendall curve iii) that the overall
381 functional design of FcγRs is adapted to physical cross-linking by soluble vs. membrane-bound
382 immune complexes. The new test system has various obvious applications in medicine and
383 pharmacy.

384

385 **A novel assay for the quantification of disease-associated as well as synthetic sICs.**

386 The new approach presents an important and implementable advancement in immunological
387 methodology as it enables the sensitive detection of receptor-activating ICs by a relatively
388 simple, scalable *in vitro* bioassay with high-throughput potential. Based on our pilot study
389 demonstrating that the sIC-mediated FcγRIII activation correlated with SLE disease markers
390 this is of great value for larger prospective clinical studies in patients with autoimmune diseases
391 such as systemic lupus erythematosus (SLE) and rheumatoid arthritis (RA), where circulating
392 ICs have long been shown to crucially contribute to tissue damage and disease manifestations
393 ^{39, 40, 55-57}. Disease-associated, endogenous sICs can also occur during infection, e.g.
394 generated after antibody-mediated destruction of pathogenic viruses or microbes or probably
395 more likely due to the oligomeric nature of numerous viral and bacterial structural proteins
396 generated e.g. by SARS-CoV2 ⁵⁸⁻⁶⁰ HIV and hepatitis B virus (HBV) infection, during which
397 circulating sICs are generated ^{36, 61}.

398 As the assay also enables the sensitive and quantitative measurement of FcγR ligand
399 bioactivity it allows the detection of sICs not only in clinical specimens but also pharmaceutical
400 preparations of IgG and Fc-fusion proteins for therapeutic use ⁴⁵. The presence of ICs in
401 therapeutic preparations or sIC formation following patient treatment is unwanted due to the

402 risk of side effects such as lupus-like syndrome which has been linked to mAb treatment in
403 patients receiving infliximab ⁶² or bevacizumab ⁶³, both mAbs used in this study. As this assay
404 is highly sensitive to any aggregation of IgG, it also represents a tool to control the purity,
405 quality and stability of mAb preparations produced for therapeutic use in patients. In addition,
406 the assessment of sIC-mediated FcγR activation allows for optimization of mAbs and Fc-fusion
407 proteins regarding their molecular design and manufacturing. Specifically, Fc-molecules
408 targeting cytokines and soluble factors, which result in sIC formation, could be designed for
409 reduced or enhanced FcγR activation such as glyco-engineered mAbs or LALA-mutant mAbs
410 ^{64, 65}. Notably, the scalability of this cell-based test system does allow for large-scale screening
411 of samples.

412

413 **sICs form FcγR ligands with distinct functional profiles.**

414 While immobilized ICs decorating infected cells, viral particles or microbial surfaces restrict
415 their triggering effect to a single immune cell residing in very close vicinity, sICs can rapidly
416 disseminate reaching a high number of immune effector cells thus developing a systemic effect
417 with far reaching and long-lasting or even threatening consequences for the host as a whole.
418 This could explain the very tight control of sIC governed effector programs and the
419 unresponsiveness of activating receptors like FcγRI and IIA. We also observed a difference in
420 the response patterns for FcγRIIIA/B and FcγRII/B/C depending on the solubility of clustered
421 IgG (immobilized versus soluble ICs) which we validated for FcγRIIIA using primary human NK
422 cells (Fig. 4 and 5C). Importantly, only multimeric but not dimeric sICs can trigger FcγR
423 activation. This highlights the fundamental structural influence of the particular antigen as well
424 as the IgG molecule on sIC dimension and subsequent FcγR-mediated signal processing. The
425 ability of the here described assay to define and quantify the activation of individual FcγRs by
426 sIC ligands is not achievable using primary immune cells due to redundant immune responses
427 upon FcγR activation and complex, overlapping expression pattern of FcγRs. Finally, and in
428 contrast to primary human cells, murine BW5147 reporter cells are largely inert to human

429 cytokines, which provides a key advantage to measure FcγR activation selectively in human
430 samples.

431 Notably, the two basically sIC-responsive human FcγR types, i.e. FcγRIIIA/B and FcγRIIB, are
432 either highly activating versus strongly inhibitory and thus show a mutually exclusive
433 expression pattern (ref. review, z.B. Ravetch und Falk). FcγRIIIA mediates ADCC elicited by
434 NK cells and the induction of a pro-inflammatory cytokine profile by CD16⁺ monocytes, while
435 FcγRIIB is a GPI-anchored receptor on neutrophils. FcγRIIB is an inhibitory receptor
436 expressed by B cells and dendritic cells (DCs) regulating B cell activation, antibody production
437 by plasma cells and the activation state of DCs, while the activating FcγRIIC is found on NK
438 cells mediating ADCC. However, as FcγRIIC is only expressed by roughly 10% of the human
439 population, its role is still poorly understood ⁴⁸⁻⁵¹. Given the here shown fundamental difference
440 in FcγR reactivity towards multimeric sICs versus immobilized IgG it is tempting to speculate
441 that FcγRIIIA/B- and FcγRIIB/C-positive immune cells might have evolved to differentially
442 perceive these different FcγR ligands (sICs versus membrane bound insoluble ICs) and
443 translate them into distinct reaction patterns. This could be achieved by differences in receptor
444 density, signal transduction or regulation of receptor expression. Consulting the literature
445 indeed supports our hypothesis with neutrophils, B cells and NK cells being efficiently activated
446 by sICs via essentially identical receptor ectodomains ^{18, 28, 66, 67}, while the immunological
447 outcome of their triggering very much differs.

448

449 **Revisiting the Heidelberger-Kendall curve: dynamic sIC size measurement and** 450 **monitoring of bioactivity in sIC-associated diseases.**

451 We provide for the first time a simultaneous functional and biophysical assessment of the
452 paradigmatic Heidelberger-Kendall precipitation curve ^{12, 13}. While previous work already
453 revealed that large and small sICs differentially impacts IL-6 production in PBMCs ⁶, the
454 dynamics of FcγR activation resulting from constant changes in sIC size have not been
455 explored on a systematic basis. This was undertaken in this study by directly analyzing
456 synthetic ICs formed by highly pure recombinant components via AF4 (Fig. 5A, Fig. S2, Table

457 S1). Our data document that sIC size is indeed governed by antibody:antigen ratios covering
458 a wide range of sizes up to several megadaltons. In the presence of increasing amounts of
459 antibody or antigen deviating from an optimal antibody:ratio, sIC size steadily decreases.
460 Further, by the measurement of FcγR activation we now translate sIC size directly to a simple
461 but precise read-out. In doing so, we show that sIC size essentially tunes FcγR activation on
462 and off. Thus, our new test system can not only contribute to the functional detection and
463 quantification of clinically relevant sICs but also provides a starting point on how to avoid
464 pathological consequences by influencing the sIC size, for example by administering
465 therapeutic antibodies or recombinant antigens in optimized concentrations, thus becoming
466 relevant in clinical pharmacokinetics.

467

468 **Limitations of the reporter system and conclusions**

469 While it is known that FcRIIA requires CD16B or FcRn to efficiently respond to ICs ^{22, 23, 68},
470 unexpectedly, we found that FcγRI is not activated by sICs in our assay. We assume that FcγRI
471 interaction with sICs might require a native cellular environment given that a major function of
472 this FcγR is the uptake and processing of antigen via ICs even in the absence of a signaling
473 motif ²¹. However, we find that FcγRI ectodomains alone are not responsive to sICs implying
474 a thoroughly different cross-linking threshold for FcγRI compared with FcγRIIB and IIIA/B. This
475 feature is possibly linked to its molecular architecture being the only high-affinity FcγR with
476 three extracellular Ig domains compared to the two domains found in other FcγRs with lower
477 affinity to monomeric IgG. This observation also reflects a general consideration regarding the
478 BW5147 reporter system. While providing a robust and uniform read-out using a scalable cell-
479 based approach, the assay is not able to reflect native immune cell functions governed by cell-
480 intrinsic signalling cascades. The major advancements of this reporter system include i) a
481 higher accuracy regarding FcγR activation compared to merely affinity measurements, ii) an
482 sIC size dependent quantification of FcγR responsiveness and iii) the identification of FcγR
483 activating sICs in autoimmunity and infection. Finally, this scalable, sensitive and robust

484 system to detect FcγR activating sICs in clinical samples might enable their identification in
485 diseases that have not been linked to sIC-mediated pathology, yet.

486

487

488 **Materials and Methods**

489

490 **Cell culture**

491 All cells were cultured in a 5% CO₂ atmosphere at 37°C. BW5147 mouse thymoma cells (BW,
492 obtained from ATCC: TIB-47) were maintained at 3x10⁵ to 9x10⁵ cells/ml in Roswell Park
493 Memorial Institute medium (RPMI GlutaMAX, Gibco) supplemented with 10% (vol/vol) fetal calf
494 serum (FCS, Biochrom), sodium pyruvate (1x, Gibco) and β-mercaptoethanol (0.1 mM, Gibco).
495 293T-CD20 (kindly provided by Irvin Chen, UCLA ⁶⁹) were maintained in Dulbecco's modified
496 Eagle's medium (DMEM, Gibco) supplemented with 10% (vol/vol) FCS.

497

498 **FcγR receptor activation assay**

499 FcγR activation was measured adapting a previously described cell-based assay ^{44, 70}. The
500 assay was modified to measure FcγR activation in solution. Briefly, 2x10⁵ mouse BW-FcγR
501 (BW5147) reporter cells were incubated with synthetic sICs or diluted serum in a total volume
502 of 100 μl for 16 h at 37°C and 5% CO₂. Incubation was performed in a 96-well ELISA plate
503 (Nunc maxisorp) pre-treated with PBS/10% FCS (v/v) for 1 h at 4°C. Immobilized IgG was
504 incubated in PBS on the plates prior to PBS/10% FCS treatment. Reporter cell mIL-2 secretion
505 was quantified via ELISA as described ⁴⁴.

506

507 **Recombinant antigens and monoclonal antibodies to form sICs**

508 Recombinant human (rh) cytokines TNF, IL-5, and VEGFA were obtained from Stem Cell
509 technologies. Recombinant CD20 was obtained as a peptide (aa141-188) containing the
510 binding region of rituximab (Creative Biolabs). FcγR-specific mAbs were obtained from Stem
511 Cell technologies (CD16: clone 3G8; CD32: IV.3). Reverse sICs were generated from these

512 receptor-specific antibodies using goat-anti-mouse IgG F(ab)₂ fragments (Invitrogen) in a 1:1
513 ratio. Pharmaceutically produced humanized monoclonal IgG1 antibodies infliximab (Ifx),
514 bevacizumab (Bvz), mepolizumab (Mpz) and rituximab (Rtx) were obtained from the University
515 Hospital Pharmacy Freiburg. Mouse anti-hTNF α (IgG2b, R&D Systems, 983003) was used to
516 generate sICs reactive with mouse Fc γ Rs. sICs were generated by incubation of antigens and
517 antibodies in reporter cell medium or PBS for 2 h at 37°C.

518

519 **Lentiviral transduction**

520 Lentiviral transduction of BW5147 cells was performed as described previously^{46, 54}. In brief,
521 chimeric Fc γ R-CD3 ζ constructs⁴⁴ were cloned into a pUC2CL6IPwo plasmid backbone. For
522 every construct, one 10-cm dish of packaging cell line at roughly 70% density was transfected
523 with the target construct and two supplementing vectors providing the VSV gag/pol and VSV-
524 G-env proteins (6 μ g of DNA each) using polyethylenimine (22.5 μ g/ml, Sigma) and Polybrene
525 (4 μ g/ml; Merck Millipore) in a total volume of 7 ml (2 ml of a 15-min-preincubated transfection
526 mix in serum-free DMEM added to 5 ml of fresh full DMEM). After a medium change, virus
527 supernatant harvested from the packaging cell line 2 days after transfection was then
528 incubated with target BW cells overnight (3.5 ml of supernatant on 10⁶ target cells), followed
529 by expansion and pool selection using complete medium supplemented with 2 μ g/ml of
530 puromycin (Sigma) over a one week culture period.

531

532 **BW5147 toxicity test**

533 Cell counting was performed using a Countess II (Life Technologies) according to supplier
534 instructions. Cell toxicity was measured as a ratio between live and dead cells judged by trypan
535 blue staining over a 16 h time frame in a 96well format (100 μ l volume per well). BW5147 cells
536 were mixed 1:1 with Trypan blue (Invitrogen) and analysed using a Countess II. rhTNF α was
537 diluted in complete medium.

538

539 **human IgG suspension ELISA**

540 1 µg of IgG1 (rituximab in PBS, 50 µl/well) per well was incubated on a 96well microtiter plate
541 (NUNC Maxisorp) pre-treated (2h at RT) with PBS supplemented with varying percentages
542 (v/v) of FCS (PAN Biotech). IgG1 bound to the plates was detected using an HRP-conjugated
543 mouse-anti-human IgG mAb (Jackson ImmunoResearch).

544

545 **BW5147 cell flow cytometry**

546 BW5147 cells were harvested by centrifugation at 900 g and RT from the suspension culture.
547 1×10^6 cells were stained with PE- or FITC-conjugated anti-human FcγR mAbs (BD) or a PE-
548 TexasRed-conjugated human IgG-Fc fragment (Rockland) for 1h at 4°C in PBS/3%FCS. After
549 3 washing steps in PBS/3%FCS, the cells were transferred to Flow cytometry tubes (BD) and
550 analysed using BD LSR Fortessa and FlowJo (V10) software.

551

552 **NK cell activation flow cytometry**

553 PBMC were purified from donor blood using Lymphocyte separation Media (Anprotec). Primary
554 NK cells were separated from donor PBMCs via magnetic bead negative selection (Stem Cell
555 technologies) and NK cell purity was confirmed via staining of CD3 (Biolegend, clone HIT3a),
556 CD16 (Biolegend, clone 3G8) and CD56 (Miltenyi Biotec, clone AF12-7H3). 96well ELISA
557 plates (Nunc Maxisorp) were pre-treated with PBS/10% FCS (v/v) for 1 h at 4°C. NK cells were
558 stimulated in pre-treated plates and incubated at 37°C and 5% CO₂ for 4 h. Golgi Plug and
559 Golgi Stop solutions (BD) were added as suggested by supplier. CD107a (APC, BD, H4A3)
560 specific conjugated mAb was added at the beginning of the incubation period. Following the
561 stimulation period, MIP-1β (PE, BD Pharmigen), IFNγ (BV-510, Biolegends, 4SB3) and TNFα
562 (PE/Cy7, Biolegends, MAB11) production was measured via intracellular staining Cytokines
563 (BD, CytoFix/CytoPerm, Kit as suggested by the supplier). 50 ng/ml PMA (InvivoGen) + 0.5
564 µM Ionomycin (InvivoGen) were used as a positive stimulation control for NK cell activation.
565 After 3 washing steps in PBS/3%FCS, the cells were transferred to Flow cytometry tubes (BD)
566 and analysed using a BD FACS Fortessa and FlowJo (V10) software. FcγRII or FcγRIII block
567 was performed by addition of receptor specific mAbs (Stem cell technologies, IV.3 and 3G8)

568 at a 1:100 dilution at the beginning of the incubation period. Cells were transferred to Flow
569 cytometry tubes (BD) and analyzed using BD LSR Fortessa and FlowJo (V10) software.

570

571 **Asymmetric flow field flow fractionation (AF4)**

572 The AF4 system consisted of a flow controller (Eclipse AF4, Wyatt), a MALS detector (DAWN
573 Heleos II, Wyatt), a UV detector (1260 Infinity G1314F, Agilent) and the separation channel
574 (SC channel, PES membrane, cut-off 10 kDa, 490 μ m spacer, wide type, Wyatt). Elution buffer:
575 1.15 g/L Na_2HPO_4 (Merck), 0.20 g/L $\text{NaH}_2\text{PO}_4 \times \text{H}_2\text{O}$ (Merck), 8.00 g/L NaCl (Sigma) and 0,20
576 g/L NaN_3 (Sigma), adjusted to pH 7.4, filtered through 0.1 μ m. AF4 sequence (V_x = cross flow
577 in mL/min): (a) elution (2 min, V_x : 1.0); (b) focus (1 min, V_x : 1.0), focus + inject (1 min, V_x : 1.0,
578 inject flow: 0.2 mL/min), repeated three times; (c) elution (30 min, linear V_x gradient: 1.0 to
579 0.0); (d) elution (15 min, V_x : 0.0); (e) elution + inject (5 min, V_x : 0.0). A total protein mass of
580 $17 \pm 0.3 \mu\text{g}$ (Ifx, rhTNF α or ICs, respectively) was injected. The eluted sample concentration
581 was calculated from the UV signal at 280 nm using extinction coefficients of 1.240 mL/(mg cm)
582 or 1.450 mL/(mg cm) in the case of TNF α or Ifx, respectively. For the ICs, extinction coefficients
583 were not available and difficult to calculate as the exact stoichiometry is not known. An
584 extinction coefficient of 1.450 mL/(mg cm) was used for calculating the molar masses of all
585 ICs. Especially in the case of ICs rich in TNF α , the true coefficients should be lower, and the
586 molar masses of these complexes are overestimated by not more than 14 %. The determined
587 molar masses for TNF α -rich complexes are therefore biased but the observed variations in
588 molar mass for the different ICs remain valid. The mass-weighted mean of the distribution of
589 molar masses for each sample was calculated using the ASTRA 7 software package (Wyatt).

590

591 **SLE patient cohort**

592 Sera from patients with SLE were obtained from the Immunologic, Rheumatologic Biobank (IR-
593 B) of the Department of Rheumatology and Clinical Immunology. Biobanking and the project
594 were approved by the local ethical committee of the University of Freiburg (votes 507/16 and
595 624/14). All patients who provided blood to the biobank had provided written informed consent.

596 Ethical Statement: The study was designed in accordance with the guidelines of the
597 Declaration of Helsinki (revised 2013). Patients with SLE ($n = 25$) and healthy controls ($n = 4$)
598 were examined. All patients met the revised ACR classification criteria for SLE. Disease activity
599 was assessed using the SLEDAI-2K score. C3d levels were analyzed in EDTA plasma using
600 rocket double decker immune-electrophoresis with antisera against C3d (Polyclonal Rabbit
601 Anti-Human C3d Complement, Agilent) and C3c (Polyclonal Rabbit Anti-Human C3c
602 Complement Agilent) as previously described ⁷¹. Anti-human dsDNA antibodies titers were
603 determined in serum using an anti-dsDNA IgG ELISA kit (diagnostik-a GmbH).

604

605 **Patient serum IC precipitation**

606 For polyethylene glycol (PEG) precipitation human sera were mixed with PEG 6000 (Sigma-
607 Aldrich) in PBS at a final concentration of 10% PEG 6000. After overnight incubation at 4°C,
608 ICs were precipitated by centrifugation at 2000 x g for 30 min at 4 °C, pellets were washed
609 once with PEG 6000 and then centrifugated at 2000 x g for 20 min at 4 °C. Supernatants were
610 harvested and precipitates re-suspended in pre-warmed PBS for 1 h at 37 °C. IgG
611 concentrations of serum, precipitates and supernatants obtained after precipitation were
612 quantified by Nanodrop (Thermo Scientific™) measurement.

613

614 **Mice and Models**

615 Animal experiments were approved by the local governmental commission for animal
616 protection of Freiburg (Regierungspräsidium Freiburg, approval no. G16/59 and G19/21).
617 Lupus-prone (NZBxNZW)F1 mice (NZB/WF1) were generated by crossing NZB/BINJ mice with
618 NZW/LacJ mice, purchased from The Jackson Laboratory. KRNg mice were obtained from F.
619 Nimmerjahn (Universität Erlangen-Nürnberg) with the permission of D. Mathis and C. Benoist
620 (Harvard Medical School, Boston, MA), C57BL/6 mice (BL/6) and NOD/ShiLtJArc (NOD/Lt)
621 mice were obtained from the Charles River Laboratories. K/BxN (KRNgxNOD)F1 mice
622 (K/BxN) were obtained by crossing KRNg mice and NOD/Lt mice. All mice were housed in a
623 12-h light/dark cycle, with food and water ad libitum. Mice were euthanized and blood collected

624 for serum preparation from 16 weeks old BL/6 animals, from 16 weeks old arthritic K/BxN
625 animals and from 26 – 38 weeks old NZB/WF1 mice with established glomerulonephritis.

626

627 **Statistical analyses**

628 Statistical analyses were performed using Graphpad Prism software (v6) and appropriate
629 tests.

630

631 **Funding**

632 This work was supported by an intramural junior investigator fund of the Faculty of Medicine
633 to PK (EQUIP - Funding for Medical Scientists, Faculty of Medicine, University of Freiburg), by
634 the German Research foundation (DFG) (FOR2830 HE 2526/9-1) to HH, by the DFG research
635 grant TRR130 to REV and the Ministry of Science, Research, and Arts Baden-Württemberg
636 (Margarete von Wrangell Programm) to NC.

637

638 **Acknowledgement**

639 We thank T. Schleyer (IR-B Biobank) for providing patient samples. We are indebted to Falk.
640 Nimmerjahn (Universität Erlangen-Nürnberg) for providing KRNtg mice.

641

642 **Competing interests**

643 We declare no financial and non-financial competing interests.

644

645

646 **References**

- 647 1. Lu, L.L., Suscovich, T.J., Fortune, S.M. & Alter, G. Beyond binding: antibody effector
648 functions in infectious diseases. *Nat Rev Immunol* **18**, 46-61 (2018).
- 649 2. Ravetch, J.V. & Bolland, S. IgG Fc receptors. *Annu Rev Immunol* **19**, 275-290 (2001).
- 650 3. van der Poel, C.E., Spaapen, R.M., van de Winkel, J.G. & Leusen, J.H. Functional
651 characteristics of the high affinity IgG receptor, FcγRI. *J Immunol* **186**, 2699-
652 2704 (2011).
- 653 4. Bruhns, P. et al. Specificity and affinity of human Fcγ receptors and their
654 polymorphic variants for human IgG subclasses. *Blood* **113**, 3716-3725 (2009).
- 655 5. Urlaub, D. et al. Activation of natural killer cells by rituximab in granulomatosis with
656 polyangiitis. *Arthritis Res Ther* **21**, 277 (2019).
- 657 6. Lux, A., Yu, X., Scanlan, C.N. & Nimmerjahn, F. Impact of immune complex size and
658 glycosylation on IgG binding to human FcγRs. *J Immunol* **190**, 4315-4323
659 (2013).
- 660 7. Kiefer, F. et al. The Syk protein tyrosine kinase is essential for Fc gamma receptor
661 signaling in macrophages and neutrophils. *Mol Cell Biol* **18**, 4209-4220 (1998).
- 662 8. Luo, Y., Pollard, J.W. & Casadevall, A. Fcγ receptor cross-linking stimulates cell
663 proliferation of macrophages via the ERK pathway. *J Biol Chem* **285**, 4232-4242
664 (2010).
- 665 9. Greenberg, S., Chang, P. & Silverstein, S.C. Tyrosine phosphorylation of the gamma
666 subunit of Fc gamma receptors, p72syk, and paxillin during Fc receptor-mediated
667 phagocytosis in macrophages. *J Biol Chem* **269**, 3897-3902 (1994).
- 668 10. Bournazos, S., Wang, T.T., Dahan, R., Maamary, J. & Ravetch, J.V. Signaling by
669 Antibodies: Recent Progress. *Annu Rev Immunol* **35**, 285-311 (2017).
- 670 11. Nimmerjahn, F. & Ravetch, J.V. Antibody-mediated modulation of immune responses.
671 *Immunol Rev* **236**, 265-275 (2010).
- 672 12. Heidelberger, M. & Kendall, F.E. A Quantitative Study of the Precipitin Reaction
673 between Type Iii Pneumococcus Polysaccharide and Purified Homologous Antibody. *J*
674 *Exp Med* **50**, 809-823 (1929).
- 675 13. Heidelberger, M. & Kendall, F.E. The Precipitin Reaction between Type Iii
676 Pneumococcus Polysaccharide and Homologous Antibody : Iii. A Quantitative Study
677 and a Theory of the Reaction Mechanism. *J Exp Med* **61**, 563-591 (1935).
- 678 14. Duchemin, A.M., Ernst, L.K. & Anderson, C.L. Clustering of the High-Affinity Fc
679 Receptor for Immunoglobulin-G (Fc-γ-Ri) Results in Phosphorylation of Its
680 Associated γ-Chain. *J Biol Chem* **269**, 12111-12117 (1994).
- 681 15. Getahun, A. & Cambier, J.C. Of ITIMs, ITAMs, and ITAMis: revisiting immunoglobulin
682 Fc receptor signaling. *Immunol Rev* **268**, 66-73 (2015).
- 683 16. Bruhns, P. & Jonsson, F. Mouse and human FcR effector functions. *Immunol Rev* **268**,
684 25-51 (2015).
- 685 17. Bruhns, P. Properties of mouse and human IgG receptors and their contribution to
686 disease models. *Blood* **119**, 5640-5649 (2012).
- 687 18. Nimmerjahn, F. & Ravetch, J.V. Fcγ receptors as regulators of immune
688 responses. *Nat Rev Immunol* **8**, 34-47 (2008).
- 689 19. Nimmerjahn, F. & Ravetch, J.V. Fcγ receptors: old friends and new family
690 members. *Immunity* **24**, 19-28 (2006).
- 691 20. Williams, M., Bruhns, P., Saeys, Y., Hammad, H. & Lambrecht, B.N. The function of
692 Fcγ receptors in dendritic cells and macrophages. *Nat Rev Immunol* **14**, 94-108
693 (2014).
- 694 21. Indik, Z.K. et al. The high affinity Fc gamma receptor (CD64) induces phagocytosis in
695 the absence of its cytoplasmic domain: the gamma subunit of Fc gamma RIIIA imparts
696 phagocytic function to Fc gamma RI. *Exp Hematol* **22**, 599-606 (1994).
- 697 22. Fossati, G., Bucknall, R.C. & Edwards, S.W. Insoluble and soluble immune complexes
698 activate neutrophils by distinct activation mechanisms: changes in functional responses
699 induced by priming with cytokines. *Ann Rheum Dis* **61**, 13-19 (2002).

- 700 23. Hubbard, J.J. et al. FcRn is a CD32a coreceptor that determines susceptibility to IgG
701 immune complex-driven autoimmunity. *J Exp Med* **217** (2020).
- 702 24. Pincetic, A. et al. Type I and type II Fc receptors regulate innate and adaptive immunity.
703 *Nat Immunol* **15**, 707-716 (2014).
- 704 25. Vidarsson, G., Dekkers, G. & Rispens, T. IgG subclasses and allotypes: from structure
705 to effector functions. *Front Immunol* **5**, 520 (2014).
- 706 26. Tay, M.Z., Wiehe, K. & Pollara, J. Antibody-Dependent Cellular Phagocytosis in
707 Antiviral Immune Responses. *Front Immunol* **10**, 332 (2019).
- 708 27. Laborde, E.A. et al. Immune complexes inhibit differentiation, maturation, and function
709 of human monocyte-derived dendritic cells. *J Immunol* **179**, 673-681 (2007).
- 710 28. Kang, S. et al. IgG-Immune Complexes Promote B Cell Memory by Inducing BAFF. *J*
711 *Immunol* **196**, 196-206 (2016).
- 712 29. Granger, V., Peyneau, M., Chollet-Martin, S. & de Chaisemartin, L. Neutrophil
713 Extracellular Traps in Autoimmunity and Allergy: Immune Complexes at Work. *Front*
714 *Immunol* **10**, 2824 (2019).
- 715 30. Berger, S., Ballo, H. & Stutte, H.J. Immune complex-induced interleukin-6, interleukin-
716 10 and prostaglandin secretion by human monocytes: A network of pro- and anti-
717 inflammatory cytokines dependent on the antigen:antibody ratio. *Eur J Immunol* **26**,
718 1297-1301 (1996).
- 719 31. Koenderman, L. Inside-Out Control of Fc-Receptors. *Front Immunol* **10**, 544 (2019).
- 720 32. Plomp, R. et al. Subclass-specific IgG glycosylation is associated with markers of
721 inflammation and metabolic health. *Sci Rep* **7**, 12325 (2017).
- 722 33. Pierson, T.C. et al. The stoichiometry of antibody-mediated neutralization and
723 enhancement of West Nile virus infection. *Cell Host Microbe* **1**, 135-145 (2007).
- 724 34. Patel, K.R., Roberts, J.T. & Barb, A.W. Multiple Variables at the Leukocyte Cell Surface
725 Impact Fc gamma Receptor-Dependent Mechanisms. *Front Immunol* **10**, 223 (2019).
- 726 35. Bohm, S., Kao, D. & Nimmerjahn, F. Sweet and sour: the role of glycosylation for the
727 anti-inflammatory activity of immunoglobulin G. *Current topics in microbiology and*
728 *immunology* **382**, 393-417 (2014).
- 729 36. Wang, T.T. & Ravetch, J.V. Immune complexes: not just an innocent bystander in
730 chronic viral infection. *Immunity* **42**, 213-215 (2015).
- 731 37. Yamada, D.H. et al. Suppression of Fc gamma-receptor-mediated antibody effector
732 function during persistent viral infection. *Immunity* **42**, 379-390 (2015).
- 733 38. Antes, U., Heinz, H.P., Schultz, D., Brackertz, D. & Loos, M. C1q-bearing immune
734 complexes detected by a monoclonal antibody to human C1q in rheumatoid arthritis
735 sera and synovial fluids. *Rheumatol Int* **10**, 245-250 (1991).
- 736 39. Zubler, R.H. et al. Circulating and intra-articular immune complexes in patients with
737 rheumatoid arthritis. Correlation of 125I-C1q binding activity with clinical and biological
738 features of the disease. *J Clin Invest* **57**, 1308-1319 (1976).
- 739 40. Koffler, D., Agnello, V., Thoburn, R. & Kunkel, H.G. Systemic lupus erythematosus:
740 prototype of immune complex nephritis in man. *J Exp Med* **134**, 169-179 (1971).
- 741 41. Rajan, T.V. The Gell-Coombs classification of hypersensitivity reactions: a re-
742 interpretation. *Trends in immunology* **24**, 376-379 (2003).
- 743 42. Tahir, S. et al. A CD153+CD4+ T follicular cell population with cell-senescence features
744 plays a crucial role in lupus pathogenesis via osteopontin production. *J Immunol* **194**,
745 5725-5735 (2015).
- 746 43. Bano, A. et al. CD28 (null) CD4 T-cell expansions in autoimmune disease suggest a
747 link with cytomegalovirus infection. *F1000Res* **8** (2019).
- 748 44. Corrales-Aguilar, E. et al. A novel assay for detecting virus-specific antibodies
749 triggering activation of Fc gamma receptors. *Journal of immunological methods* **387**,
750 21-35 (2013).
- 751 45. Lagasse, H.A.D., Hengel, H., Golding, B. & Sauna, Z.E. Fc-Fusion Drugs Have
752 Fc gamma R/C1q Binding and Signaling Properties That May Affect Their
753 Immunogenicity. *AAPS J* **21**, 62 (2019).

- 754 46. Van den Hoecke, S. et al. Hierarchical and Redundant Roles of Activating FcγRI in Protection against Influenza Disease by M2e-Specific IgG1 and IgG2a Antibodies. *J Virol* **91** (2017).
- 755
- 756
- 757 47. Tanaka, M. et al. Activation of FcγRI on monocytes triggers differentiation into immature dendritic cells that induce autoreactive T cell responses. *J Immunol* **183**, 2349-2355 (2009).
- 758
- 759
- 760 48. Lisi, S., Sisto, M., Lofrumento, D.D., D'Amore, S. & D'Amore, M. Advances in the understanding of the Fcγ receptors-mediated autoantibodies uptake. *Clin Exp Med* **11**, 1-10 (2011).
- 761
- 762
- 763 49. Anania, J.C., Chenoweth, A.M., Wines, B.D. & Hogarth, P.M. The Human FcγRII (CD32) Family of Leukocyte FcR in Health and Disease. *Front Immunol* **10**, 464 (2019).
- 764
- 765 50. Metes, D. et al. Expression of functional CD32 molecules on human NK cells is determined by an allelic polymorphism of the FcγRIIC gene. *Blood* **91**, 2369-2380 (1998).
- 766
- 767
- 768 51. Breunis, W.B. et al. Copy number variation of the activating FCGR2C gene predisposes to idiopathic thrombocytopenic purpura. *Blood* **111**, 1029-1038 (2008).
- 769
- 770 52. Vuckovic, F. et al. Association of systemic lupus erythematosus with decreased immunosuppressive potential of the IgG glycome. *Arthritis Rheumatol* **67**, 2978-2989 (2015).
- 771
- 772
- 773 53. Kaneko, Y., Nimmerjahn, F. & Ravetch, J.V. Anti-inflammatory activity of immunoglobulin G resulting from Fc sialylation. *Science* **313**, 670-673 (2006).
- 774
- 775 54. Kolb, P. et al. Identification and Functional Characterization of a Novel Fcγ Binding Glycoprotein in Rhesus Cytomegalovirus. *J Virol* **93** (2019).
- 776
- 777 55. Nydegger, U.E. & Davis, J.S.t. Soluble immune complexes in human disease. *CRC Crit Rev Clin Lab Sci* **12**, 123-170 (1980).
- 778
- 779 56. Levinsky, R.J., Cameron, J.S. & Soothill, J.F. Serum immune complexes and disease activity in lupus nephritis. *Lancet* **1**, 564-567 (1977).
- 780
- 781 57. Levinsky, R.J. Role of circulating soluble immune complexes in disease. *Arch Dis Child* **53**, 96-99 (1978).
- 782
- 783 58. Briant, L., Coudronniere, N., Robert-Hebmann, V., Benkirane, M. & Devaux, C. Binding of HIV-1 virions or gp120-anti-gp120 immune complexes to HIV-1-infected quiescent peripheral blood mononuclear cells reveals latent infection. *J Immunol* **156**, 3994-4004 (1996).
- 784
- 785
- 786
- 787 59. Oh, S.K. et al. Identification of HIV-1 envelope glycoprotein in the serum of AIDS and ARC patients. *J Acquir Immune Defic Syndr* (1988) **5**, 251-256 (1992).
- 788
- 789 60. Vuitton, D.A., Vuitton, L., Seilles, E. & Galanaud, P. A plea for the pathogenic role of immune complexes in severe Covid-19. *Clin Immunol* **217**, 108493 (2020).
- 790
- 791 61. Madalinski, K., Burczynska, B., Heermann, K.H., Uy, A. & Gerlich, W.H. Analysis of viral proteins in circulating immune complexes from chronic carriers of hepatitis B virus. *Clin Exp Immunol* **84**, 493-500 (1991).
- 792
- 793
- 794 62. Wetter, D.A. & Davis, M.D. Lupus-like syndrome attributable to anti-tumor necrosis factor alpha therapy in 14 patients during an 8-year period at Mayo Clinic. *Mayo Clin Proc* **84**, 979-984 (2009).
- 795
- 796
- 797 63. MacDonald, D.A. et al. Aflibercept exhibits VEGF binding stoichiometry distinct from bevacizumab and does not support formation of immune-like complexes. *Angiogenesis* **19**, 389-406 (2016).
- 798
- 799
- 800 64. Saunders, K.O. Conceptual Approaches to Modulating Antibody Effector Functions and Circulation Half-Life. *Front Immunol* **10**, 1296 (2019).
- 801
- 802 65. Li, T. et al. Modulating IgG effector function by Fc glycan engineering. *Proceedings of the National Academy of Sciences of the United States of America* **114**, 3485-3490 (2017).
- 803
- 804
- 805 66. Goodier, M.R. et al. Sustained Immune Complex-Mediated Reduction in CD16 Expression after Vaccination Regulates NK Cell Function. *Front Immunol* **7**, 384 (2016).
- 806
- 807
- 808 67. Mayadas, T.N., Tsokos, G.C. & Tsuboi, N. Mechanisms of immune complex-mediated neutrophil recruitment and tissue injury. *Circulation* **120**, 2012-2024 (2009).
- 809

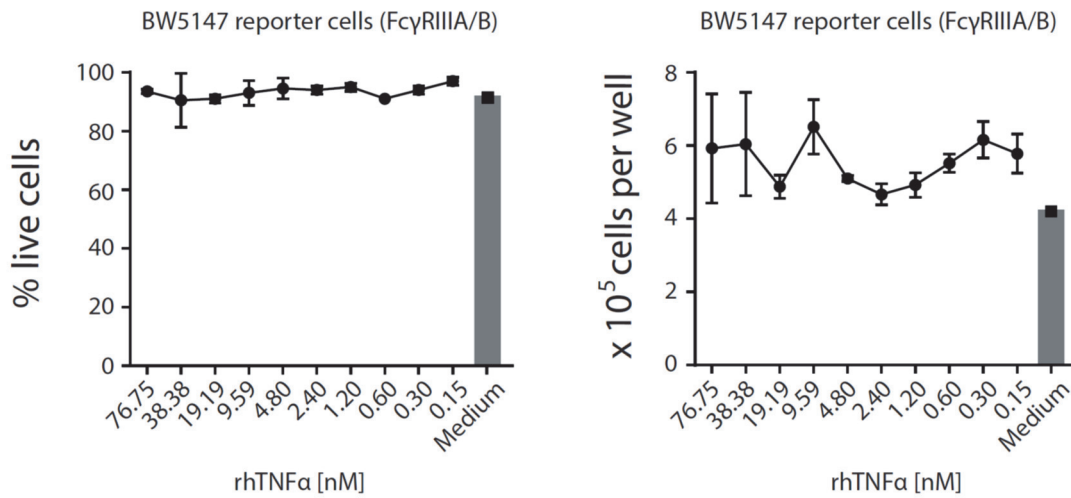
- 810 68. Nagarajan, S. et al. Cell-specific, activation-dependent regulation of neutrophil CD32A
811 ligand-binding function. *Blood* **95**, 1069-1077 (2000).
- 812 69. Morizono, K. et al. Redirecting lentiviral vectors pseudotyped with Sindbis virus-derived
813 envelope proteins to DC-SIGN by modification of N-linked glycans of envelope
814 proteins. *J Virol* **84**, 6923-6934 (2010).
- 815 70. Corrales-Aguilar, E. et al. Human cytomegalovirus Fcγ binding proteins gp34
816 and gp68 antagonize Fcγ receptors I, II and III. *PLoS pathogens* **10**, e1004131
817 (2014).
- 818 71. Rother, E., Lang, B., Coldewey, R., Hartung, K. & Peter, H.H. Complement split product
819 C3d as an indicator of disease activity in systemic lupus erythematosus. *Clin*
820 *Rheumatol* **12**, 31-35 (1993).

821

822

823 **Supplemental Data**

824

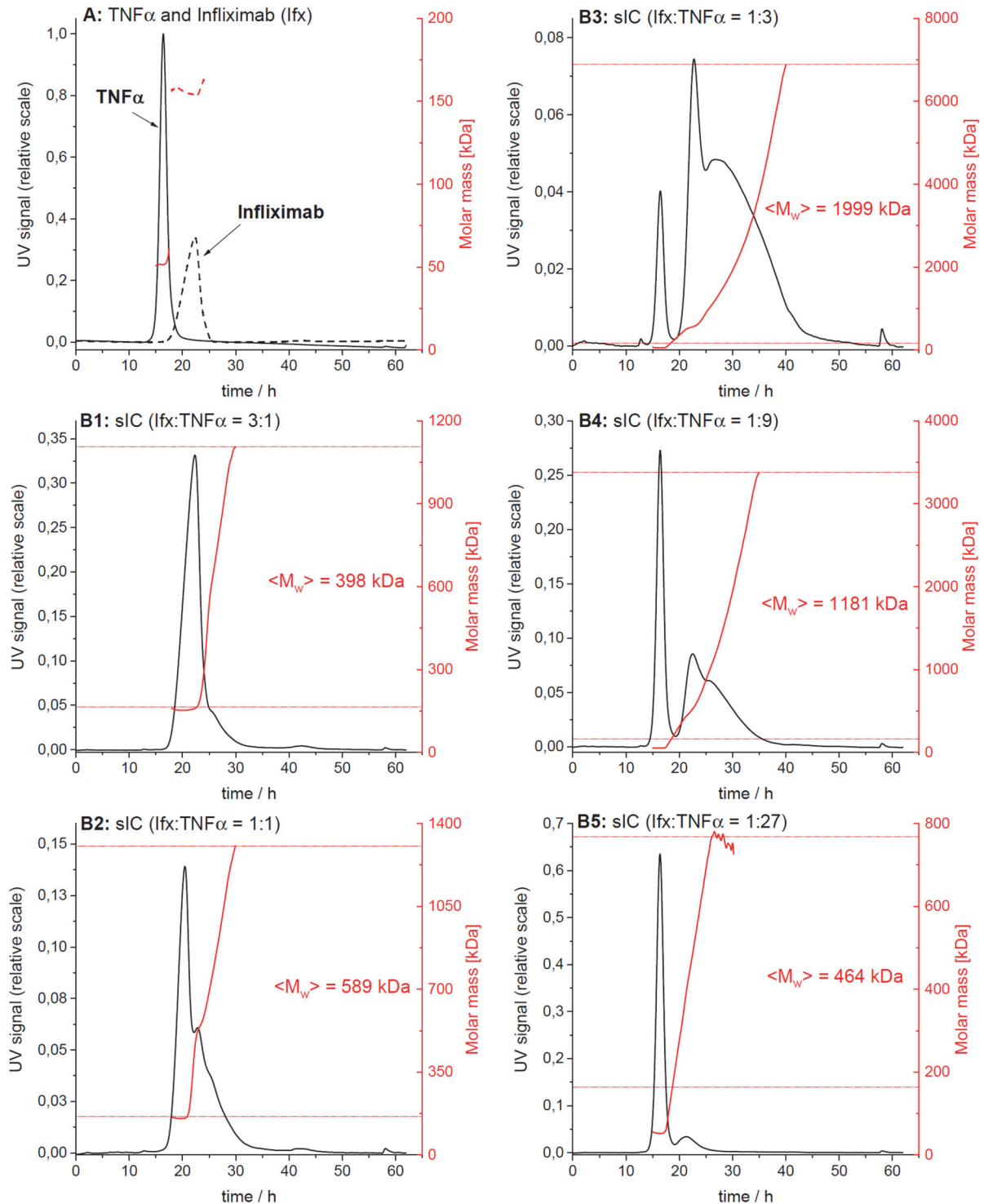


825

826 **Fig. S1. rhTNFα is not toxic to mouse lymphocyte BW5147 cells even at high**
827 **concentrations.** Cell count and percentage of live cells were unaltered over a 16 h time frame
828 of reporter cell culture in the presence of indicated rhTNFα concentrations and comparable to
829 regular growth in complete medium. Experiments were conducted in 3 replicates. Error bars =
830 SD.

831

832



833

834

Fig. S2. AF4 elution profiles of Ifx/TNF α -immune complexes.

835

The elution profiles from one of three independent runs are shown. Protein

836

concentration in the eluate is shown in black (UV signal at $\lambda = 280$ nm, normalized to

837

the highest UV signal found in this experiment), molar masses determined by MALS

838

for a given retention time in red. Horizontal red lines indicate the range of molar masses

839

used to calculate the mass-weighted mean of molar masses $\langle M_w \rangle$. A) Overlay of the

840

elution profiles obtained for TNF α and Ifx, respectively; B1 to B5) Elution profiles for

841

sICs formed after incubation of TNF α and Ifx at different molar ratios.

842

Sample	Range of assigned molar masses [kDa]			Mass-weighted mean of assigned molar masses [kDa]			
	Run 1	Run 2	Run 3	Run 1	Run 2	Run 3	Mean \pm SD
Infliximab, IFX	158 – 182	153 – 164	159 – 193	162	156	163	160 \pm 4
TNF -alpha	52 – 55	51 – 61	52 – 62	52	52	52	52 \pm 0
Immune complexes							
IFX/TNF 3:1	182 – 1.16 \cdot 10 ³	164 – 1.11 \cdot 10 ³	193 – 1.10 \cdot 10 ³	409	398	518	442 \pm 66
IFX/TNF 1:1	182 – 2.06 \cdot 10 ³	164 – 1.31 \cdot 10 ³	193 – 1.42 \cdot 10 ³	801	589	681	690 \pm 106
IFX/TNF 1:3	182 – 5.05 \cdot 10 ³	164 – 6.89 \cdot 10 ³	193 – 10.8 \cdot 10 ³	1.77 \cdot 10 ³	2.00 \cdot 10 ³	2.61 \cdot 10 ³	2.13 \cdot 10 ³ \pm 435
IFX/TNF 1:9	182 – 5.36 \cdot 10 ³	164 – 3.38 \cdot 10 ³	193 – 3.51 \cdot 10 ³	1.66 \cdot 10 ³	1.18 \cdot 10 ³	1.17 \cdot 10 ³	1.34 \cdot 10 ³ \pm 279
IFX/TNF 1:27	182 – 1.68 \cdot 10 ³	164 – 768	193 – 1.01 \cdot 10 ³	689	464	521	558 \pm 117

843
844
845
846
847
848
849
850
851
852
853

Table S1. Analysis of the molar mass distribution of ICs from AF4 data.

For a given elution time, the AF4 profiles provide the concentration (UV) at which a given molar mass (MALS) of a protein is present in the sample. The molar mass distribution of lfx, TNF α and their immune complexes (sICs) was obtained by plotting the cumulative frequency as a function of molar mass. For a selected range of molar masses, a mass-weighted mean value ($\langle M_w \rangle$) was calculated. All detected molar masses were selected in the case of lfx and TNF α whereas only molar masses larger than the maximal molar mass found for lfx were assigned to sICs. The table shows the range of assigned molar masses and the calculated $\langle M_w \rangle$ for each AF4 run (n = 3).